13th International Conference on
Structural Health Monitoring of Intelligent Infrastructure
DOI: 10.3217/978-3-99161-057-1-116

Long-term monitoring and data processing of a continuous prestressed concrete bridge

Marc Savard, PhD, Eng., Jean-François Laflamme, MSc, Eng.
Direction de la gestion des structures, Ministère des Transports et de la Mobilité durable, Québec, Canada
email: marc.savard@transports.gouv.qc.ca, jean-francois.laflamme@transports.gouv.qc.ca

ABSTRACT: The Grand-Mere Bridge in the province of Québec, Canada, built in 1977, is a cast-in-place, segmental box-girder bridge measuring 285 m (935 ft) in length. Several problems arose during the construction of this bridge and an increasing deflection combined with localized cracking were noted after only a few months of operation. These defects were mainly due to insufficient prestressing, causing high tensile stresses in the deck and possible corrosion of the prestressing steel. A few years after strengthening of the bridge in 1992, a long-term monitoring program was implemented, including vibrating wire sensors (strain and crack sensors), inclinometers and temperature sensors. So far, more than 20 years of data have been collected and processed, leading to the recommendation of the rehabilitation of the structure using stay cables to ensure that the structure performs well until its scheduled replacement. This paper presents the instrumentation strategies, the various trends observed in the data and the relevant interpretations derived from them. In the context of damage detection, finite-element models have been developed and calibrated on measurements. Data indicate that the addition of stay cables eliminated the progression of permanent deflection and provided the structural system with added strength and redundancy. Lessons learned from this investigation are presented, along with a discussion of the conditions required for successful electronic monitoring.

KEY WORDS: Bridge monitoring; Bridge modeling; Data processing; Damage detection; Bridge rehabilitation.

1 INTRODUCTION

To manage all the structures under its responsibility, the Quebec Ministère des Transports et de la Mobilité durable (MTMD) has set up a periodic visual inspection program. The purpose of these inspections is to quickly detect defects that could reduce the strength of a structure or its durability. Defects that could jeopardize the safety of a structure are considered when assessing its theoretical load-bearing capacity.

Assessing the capacity of a concrete bridge is a complex task. It is very difficult to accurately assess the impact on capacity of a specific deterioration. The loss of capacity associated with a defect depends on its nature, location and extent. Moreover, the deterioration process evolves over time, often to the detriment of structural capacity.

The manager of a structure whose theoretical load-bearing capacity is inadequate can consider various approaches. Firstly, the structure can be reinforced or rebuilt in the very short term. Since financial resources are limited, this solution is only considered for structures with the most acute defects, or when the structure's reliability in the very short term is questionable. Secondly, restrictions on bridge exploitation may be imposed, for instance, reducing the number of lanes open to traffic or limiting maximum allowable loads. In the case of many highway bridges, restrictive measures are often unacceptable. The complete closure of a bridge is also unacceptable when no detour route can be considered or when the length of the detour is important.

When the reliability of a structure is questionable, it is possible, in some cases, to extend its useful life by placing it under electronic monitoring. One of the aims of such monitoring is to gather data that can be used to determine the rate of progression of the damage process. Monitoring may focus on structural properties such as equivalent stiffness, vibration frequencies or modal damping. It is also possible to monitor the evolution of local parameters such as concrete crack width. Electronic monitoring can therefore be used to ascertain that the bridge is performing adequately under site-specific operating conditions.

Note that only slowly progressive failure modes can be properly monitored, and redundancy within the structural system is highly desirable, if not mandatory. In all cases where remote monitoring is being considered, the reliability of the structure must be ensured in the immediate future and cannot be adversely compromised by any subsequent worsening of the defects.

The Grand-Mère Bridge, in Québec, Canada, built in 1977 and measuring 285 m in length, consists of a three-span continuous prestressed concrete box girder of variable inertia. The central span is 181.4 m in length, while the two end spans are 39.6 m in length. Figure 1 shows an elevation view of the structure. At both ends of the three continuous spans and over one pier (at points B, D and E), roller supports have been chosen to allow the horizontal movement of the box girder. Pin supports are considered at the top of one pier (point C). Figure 2 illustrates cross-section geometry. Designed to limit deadweight stresses, this section depth variation does not meet current design recommendations regarding depth-to-length ratios. Another special feature of this bridge is that instead of prestressing cables, up to 216 longitudinal prestressing bars were distributed over tensioned portions of the box-girder cross section (mainly over the piers and at bottom of center span).

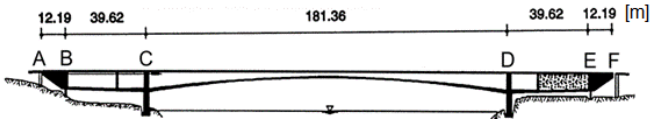

Figure 1. Elevation view of the bridge.

DOI: 10.3217/978-3-99161-057-1-116

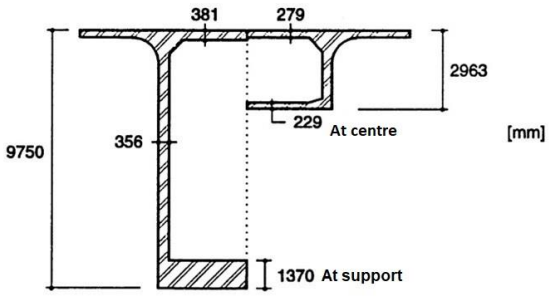

Figure 2. Cross-section geometry of the bridge.

Unfortunately, this bridge has experienced various problems resulting, among other factors, from many defects introduced during construction, such as poor quality of concrete between points B and C and the use of sleeves (joining end-to-end bars) that do not have the expected mechanical properties (many of them snapped). Also, the sheaths chosen were too tight around the prestressing bar, making grouting difficult. As a result, the prestressing bars are partially bonded to the surrounding concrete over undetermined portions of their length. Poor grouting can also lead to corrosion problems. The result of these defects is an asymmetric permanent stress distribution in the structure having a ballast at only one end of the bridge (instead of both ends, as initially designed) and additional compensating prestressing bars placed over pier C. In addition, as soon as the bridge was commissioned, a deflection at mid-span began to increase and shear cracking developed near the supports.

It has been recognized that many of the bridge's serviceability problems were due mainly to insufficient prestressing and limited knowledge at the time of design, especially regarding the estimation of creep and thermal stresses. While numerous studies showed that the short-term safety of the bridge was adequate, long-term integrity could be affected if short-term corrective measures were not taken [1]. Consequently, in 1992, the MTMD decided to strengthen the bridge by adding longitudinal prestressing cables in the box girder over piers C and D. Additional cables connected the bottom of the mid-span section of the bridge to the top of its ends. Since the deformation of the main span continued thereafter, a long-term monitoring program was initiated in 2001. The present paper briefly discusses a few of this program's findings, which led to the rehabilitation of the bridge using stay cables.

2 GENERAL CONSIDERATIONS FOR THE DESIGN OF THE BRIDGE'S STRUCTURAL HEALTH MONITORING SYSTEM

2.1 Overview

The design of an appropriate structural health monitoring (SHM) system must be tailored to the structure's behaviour under serviceability conditions. In the case of the Grand-Mère Bridge, in addition to its own weight, the dominant loads to which this structure is subjected are traffic loads and temperature variations. Traffic loads are transient loads acting over a short period of time, and fatigue problems associated with repeated loading cycles are not usually a concern for prestressed concrete bridges. Consequently, the bridge response under traffic loads is generally eliminated from long-term monitoring data. Thermal loads vary on daily and seasonal basis and have a significant impact on the structure's behaviour. Therefore, assessment of the bridge's thermal response is mandatory prior to design and implementation of a suitable SHM program.

2.2 Bridge response to thermal loads

The internal temperature variation over the depth of a given cross-section can be broken down into three components: a mean value (TM), a linear vertical temperature gradient (GT) and a self-balancing non-linear component [2]. Given its nature, the latter component does not induce internal forces and global deformation of the structure. Therefore, the bridge response to thermal loads mainly results from variations of TM and GT. To perform data analysis such as linear regression, temperature sensors ought to be recorded simultaneously with measurements characterizing the bridge's response.

The following deformations occur in a structure subjected to temperature variations:

- The natural expansion and contraction of materials following a variation in the TM; these deformations are proportional and in phase with TM variations.
- The flexure strains induced by a thermal gradient GT.

Note that the presence of concrete cracks may lead to non-uniform thermal strain distribution along the structure.

As seen on Figure 2, the thickness of cross-section components is relatively uniform, varying from 279 mm to 381 mm, except for the bottom flange, which gradually increases from 229 mm at the centre to 1,370 mm at the piers. This infers a much greater thermal inertia near supports and a delay in the thermal response of thicker components.

In addition, the Grand-Mère Bridge is a complex hyperstatic structure having roller supports partially restrained that impede the free deformation of the structure. The partial restraint at the movable supports and the continuity of the spans above the piers at point C and D of Figure 1 give rise to additional thermal strains that may not be in phase with TM and GT variations.

Given the complexity of the bridge's thermal response, a finite element (FE) model has been developed (described at section 4) to predict its behaviour under specific loads. For instance, Figure 3 shows, schematically, the bridge deformation as predicted by the model of the Grand-Mère Bridge after a drop in the mean internal box girder temperature (TM). The restraint at roller supports generate axial tensile forces and associated positive strains. Consequently, sensor readings (such as extensometers or strain gauges) are expected to increase and are therefore out of phase with TM variations. In addition, as seen on Figure 3, a decrease in the TM also implies bending of the box girder and piers. Roller support restraint is responsible for these effects on the box girder. Pier bending causes a pair of horizontal forces (red arrows) acting in opposite directions at the bottom of the box girder and contributing to the lowering of the bridge profile. This pair of forces also induces axial tensile forces and bending moments in the girder. Depending on sensor location in the structure, the corresponding axial strains may or may not be in phase with TM variations.

Figure 3. Deformation (amplified) of the structure subjected to a drop in the mean temperature (TM) in the box girder.

DOI: 10.3217/978-3-99161-057-1-116

Figure 4 presents the bridge profile predicted by the FE model of the Grand-Mère Bridge subjected to a thermal gradient (GT) developing in winter (corresponding to a cooling of top section fibres). The continuity of the spans above the piers causes non-uniform bending moments along the bridge and raising of the bridge centre. Depending on sensor location, the corresponding bending strains may or may not be in phase with GT variations. Also seen on Figure 4, a winter GT implies the bending of the piers and another pair of horizontal forces in opposite directions acting at the bottom of the box girder, which attenuates the raise of the centre of the central span. Note that these horizontal forces act in the same direction as those associated with a TM drop (as seen on Figure 3).

Figure 4. Deformation (amplified) of the structure subjected to a winter GT.

A third factor affecting bridge response to thermal variation is the lengthening or shortening of the piers. Figure 5 illustrates, schematically, the deformation of the box girder as the TM of the piers decreases, as observed in winter. As expected, the continuity of the spans gives rise to internal forces accompanying a drop in the centre of the main span and shortening of the top fibres along the entire length of the bridge. Note that temperature distribution across the width of a pier may not be uniform and might account for twisting movement of the box girder occurring over the piers.

Figure 5. Deformation (amplified) of the structure associated with a drop in mean temperature in both piers.

The Grand-Mère Bridge response to a specific profile of temperature variation is therefore the result of a combination of contributions that differ in importance from one another. The information provided by a numerical model enables a better understanding of bridge behaviour and the detection of possible damage processes.

2.3 Long-term effects

Among long-term effects that may affect this bridge, creep, shrinkage, prestress losses and concrete cracking are the main factors.

Creep, and to a lesser extent shrinkage, is a complex process that plays a major role in the gradual increase in deflection of such bridges [3]. Several models have been proposed in the literature [4] to predict the effects of creep over long periods of time. A suitable model ought to be adopted for long-term deflection and prestress losses predictions.

In prestress concrete members, prestress losses [2] can lead to cracking of fibres in tension, which may promote more prestress losses, water intrusion in the concrete mass and relaunch of creep. Passive steel rebars help control the development of cracks. Predicting crack location is difficult, and the possible addition of sensors must be anticipated when designing the monitoring system.

3 INSTRUMENTATION FOR THE STRUCTURAL HEALTH MONITORING OF THE BRIDGE

3.1 Objectives

The objectives of this SHM program were mainly to track the progression of mid-span vertical deflection and to collect information relevant to ongoing damage processes (mainly cracking, concrete delamination and spalling, corrosion, and breakage of steel tendons). As mentioned earlier, consideration of the evolution of these measurements helped in the management of the structure, to ensure user safety and bridge sustainability. During the more than 20 years of the monitoring campaign, sensors have been added, dictated by the necessity to validate and cross-check collected data, better understand bridge behaviour and detect initially unexpected progressive failure modes.

Considering the expected modes of failure of the Grand-Mère bridge and the selected structural health indicators, the SHM program features the following parameters.

3.2 Temperature measurement

Since the bridge profile and internal forces are strongly influenced by the vertical thermal gradient and the mean temperature, these parameters had to be recorded. In 2001, 24 resistance temperature detectors (RTDs) were installed at a cross-section located near the centre of the main span to measure internal temperature variations. Temperature sensors distributed over a section of the bridge allow for the calculation of the mean internal temperature as well as the thermal gradient (variation of internal temperature over the height of the section). Figure 6 presents TM and GT measured near the centre of the main span since 2001. Note the excellent performance of the monitoring system, which has experienced very few breakdowns over the past 24 years. As can be seen, GT is maximized in winter and TM and GT are almost perfectly out-of-phase. Mean temperature and vertical gradient may be useful for regression analysis of various parameters such as crack breathing, top pier rotations, etc.

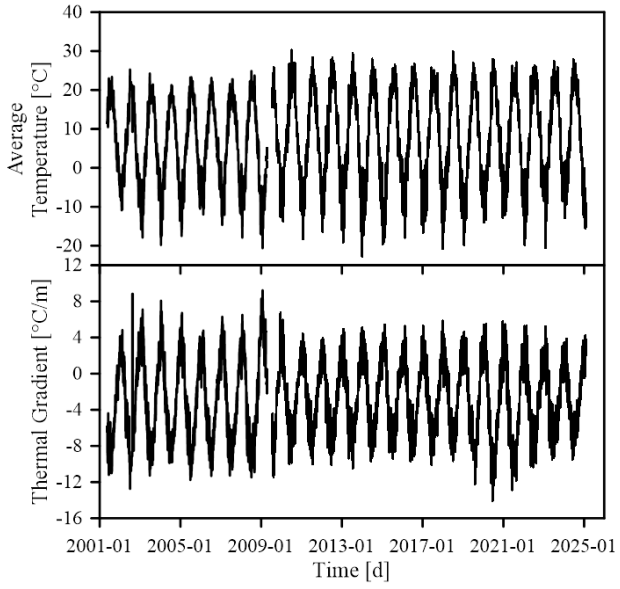

Figure 6. Internal average temperature and thermal gradient.

DOI: 10.3217/978-3-99161-057-1-116

3.3 *Estimation of mid-span deflection and box-girder torsion using tiltmeters*

To estimate vertical deflection of the main span, a total of 17 biaxial tiltmeters (sensors measuring rotation in both vertical planes) were used. Figure 7 shows the tiltmeter layout. These sensors were spaced approximately 15 m apart along the first two continuous spans. They were installed in the centre of the lower flange of the box girder. A numerical integration procedure ([7] and [8]) enables the estimation of the vertical deflection at each rotation measurement point. Measurements in the other vertical plan give indications on torsional behaviour of the box girder.

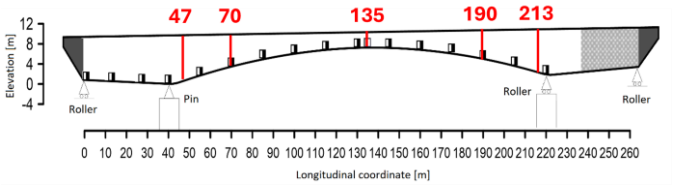

Figure 7. Tiltmeter layout and main cross-section identification.

3.4 *Strain measurement*

Thirty-two vibrating wire strain sensors located at the top and bottom of both webs allow the measurement of longitudinal strains at eight sections located in the central span at longitudinal coordinates 47, 70, 120, 125, 135, 140, 190 and 213 m. Figure 7 shows five of these sections. Figure 8 illustrates the layout of the vibrating wire sensors (VW_i). Note that these sensors are set to zero when installed, so that only strain variations are measured.

Combining a realistic value of the concrete modulus of elasticity with four longitudinal strain measurements, the variation of the four internal forces present at a measuring section (axial force, two bending moments and distortion) can be estimated [5]. Note that these calculations are made using as-built section properties and measured elastic modulus is assumed constant over time. Also, given the small size of these sensors (125 mm in length), measurements are sensitive to cracks developing nearby. Therefore, care must be taken when interpreting the data. Localization of the neutral axis (NA) is useful in this respect.

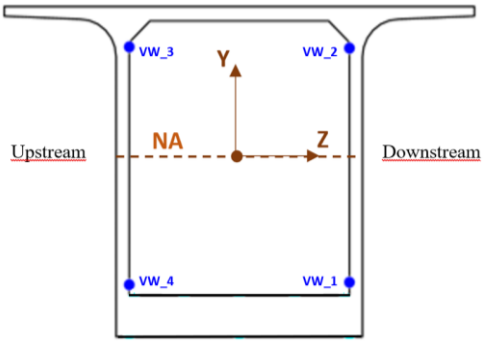

Figure 8. Typical vibrating wire sensor layout.

3.5 *Rotation and displacement at abutments and at the top of piers*

Potentiometers were installed to measure the relative horizontal movement between the box girder and supports at points B, C, D and E. Tiltmeters were also added at the top of piers at points C and D to capture pier bending. A clockwise rotation at top of piers is considered positive. These sensors aimed to assess support mobility, as discussed at section 2.2. These restraints have an impact on main span vertical deflection.

3.6 *Telescopic extensometers*

A total of eight telescopic extensometers were installed at different locations where cracks are expected in concrete. In the case of this bridge, the sensors were between 5 m and up to 6.5 m in length. These sensors measure total longitudinal displacement and axial strains occurring between their anchor points. Should a new crack (oriented generally perpendicular to sensors' axis) appear between sensor anchor points, the associated movement will be added up with the breathing of other existing cracks and the total movement will be captured by the sensors. The concrete thermal expansion response is also measured by these sensors, and only sensor thermal response is eliminated from the recordings.

Four extensometers were installed in the main span on top of the box girder close to each pier (Extenso_44 Upstream and Extenso_44 Downstream, Extenso_216 Upstream and Extenso_216 Downstream) as tension may develop in those areas prone to concrete cracks. Two other sensors were also installed outside at the bottom of the box girder near the centre of the central span (Extenso_130 Upstream and Extenso_130 Downstream), since cracks may also appear in that area. Figure 9 shows four extensometers, two that are 6.5 m long (Extenso_216) and two that are 5 m in length (Extenso_232 and Extenso_239), the latter installed under the top slab of the side-span girder.

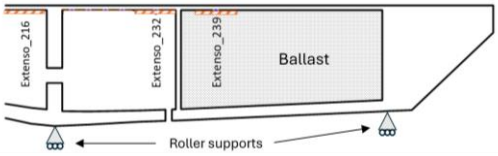

Figure 9. Telescopic extensometer layout.

4 FINITE ELEMENT MODEL

Concurrently with the SHM of the bridge, a numerical finite-element model of the crack-free structure has been developed to provide accurate estimates of expected behaviour under given load cases. Prestressing tendons were not explicitly included in the model, which means that total strain estimates are not available. However, concrete prestressing allows for the assumption of the linear and elastic behaviour of concrete, in both traction and compression areas. This assumption implies that under serviceability conditions, the largest compression stress in concrete shall never exceed 45% of concrete strength.

Moreover, prestressing forces are indirectly considered in the calibration process of the overall model. Calibration is done by adjusting the modulus of elasticity of different strategic structural components and the rigidity of the bearing devices. The objective of the calibration process is to have predicted vibration frequencies as close as possible to frequencies measured experimentally, in both bending and torsion. For instance, specific concrete properties have been established for certain portions of the webs, flanges and piers. Linear spring elements have been introduced to simulate actual support restraints. No rigidity is allocated for ballast weights.

DOI: 10.3217/978-3-99161-057-1-116

The FE model has 48,830 nodes, 27,166 parabolic 20 noded brick elements for a total of 146,465 degrees of freedom. The piers have also been modelled (embedded at their base), since their flexibility significantly influences the overall behaviour of the structure, acting like elastic supports. Figure 10 presents a general view of the model, including the stay cables and the pylons that have been designed for the rehabilitation of the structure. Tensioning of all cables was completed in September 2022.

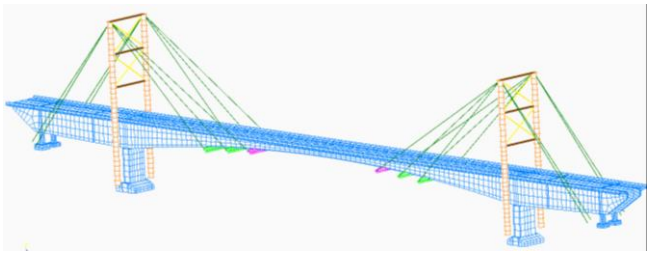

Figure 10. Isometric view of the rehabilitated bridge model.

5 DATA PROCESSING

This section presents some measurements gathered over the last 22 years with the various sensors presented above. A brief interpretation of the data is also provided.

5.1 Modal analysis and load tests

Modal analysis provides valuable information about the dynamic structural characteristics of a bridge. Recorded signals from accelerometers are analyzed and vibration frequencies and corresponding mode shapes are identified. A mode shape is a structural property that depends mainly on mass distribution and stiffness along the structure. Assuming mass remains constant over time, a change in the mode shapes or frequencies would indicate a change in rigidity resulting from cracks, concrete damage or changes to the support conditions.

A total of 12 modal analyses have been carried out at the Grand-Mère Bridge, the first one in fall 2003 and the last one in fall 2022. Since temperature affects support conditions and mode shapes, it is important to compare results under similar thermal conditions to detect damage or structural deficiencies. As reported by Cremona [6], measured frequencies may vary up to 5% for a 15°C (27°F) variation of the ambient temperature. Fall has been chosen for *in situ* modal analysis because thermal gradients are minimal during this season, thus limiting the effects of temperature on the behaviour of the structure. Vibrations have been measured under ambient traffic conditions.

Uniaxial and triaxial accelerometers individually connected to a data acquisition system have been distributed according to different schemes, for a total of 52 measuring points. The sampling frequency has been set at 200 Hz. In 2011, a wireless system was introduced, simplifying the data acquisition procedure. The location of the measuring points (schemes) has remained the same over the years. Representative results (flexural and torsional modes) of these modal analyses are gathered in Table 1.

Comparing the results for 2003 with those for 2021 at approximately the same internal temperature, a very slight decrease of the first seven frequencies of vibration is noted under normal traffic conditions. Those small variations may be caused by the thermal response of the structure, which affects support conditions and internal forces, and are not necessarily the result of a damage process. In fact, the state of stress associated with thermal variations also depends on the weather conditions on the days preceding the *in-situ* modal analysis.

To assess seasonal temperature changes on the bridge behaviour, Figure 11 presents variations of the fundamental frequency of vibration (Flex.1 in Table 1) of the bridge along with TM as a function of time. The frequency is minimal in summer (approximately 1.02 Hz) and maximal in winter (around 1.07 Hz). Bridge response to thermal variations indicates that roller supports are partially restrained and incidental bridge internal forces have an influence on modal frequencies.

Structural rigidity has also been assessed through load testing. A total of eight load tests were performed in November of each of the following years: 2008, 2012, 2013, 2018 and each year thereafter until 2022. Load tests are intended to acquire data when the bridge is solely loaded by truck loads of known intensity. Generally, the loads consisted of semi-trailer trucks of about 40 tons each, for a total load never exceeding bridge service load. Measured data are used to validate the proper functioning of all sensors and provide valuable insight for FE model calibration.

The number of trucks and their relative position on the deck varied according to predefined load cases. Associated longitudinal and lateral force distribution in the structure can be established and bridge symmetry under symmetric loading conditions may be ascertained. The linearity of the bridge response under increasing loads is also verified and upon unloading, recordings indicate if the bridge returns to its initial profile. Detailed analysis of the test measurements showed that no significant changes in structural rigidity were detected from one year to the next, even with the seasonal support restraints above-mentioned.

Table 1. Measured frequencies [Hz] of some bridge's modes.

Modes	FE model estimates	Nov. 2003	June 2013	Nov. 2021
Mean temp.		1.5°C	20.4°C	1.0°C
Flex. 1	1,038	1,034	1,024	1,025
Flex. 2	2,177	2,134	2,117	2,124
Flex. 3	3,644	3,712	3,668	3,687
Tor. 1	4,625	4,665	4,605	4,639
Flex. 4	5,498	5,664	5,551	5,615
Tor. 2	6,794	7,102	6,966	7,056
Flex. 5	7,441	7,480	7,444	7,397

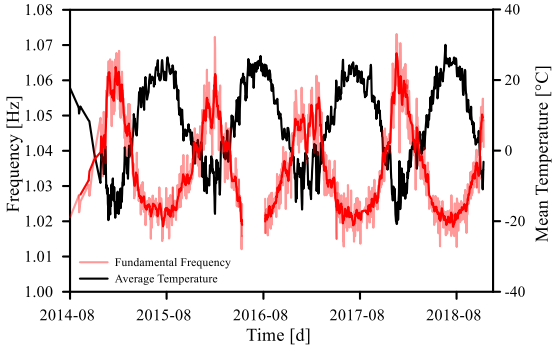

Figure 11. Variation of the fundamental frequency of vibration.

DOI: 10.3217/978-3-99161-057-1-116

5.2 *Tracking of roller support longitudinal movements and top of pier rotations*

This section presents longitudinal movements recorded at each support. Figure 12 illustrates longitudinal support movement as a function of time. The dotted line added in many figures indicates when the stay cables have been tensioned. Very small relative movements are recorded at point C where a pin support is present. Maximum annual values are occurring in winter, as expected. Figure 13 shows top of piers rotations. Rotation recordings made at point C are the counterpart of those made at point D. Also, minimum rotation measurements at top of pier D occur in winter, as predicted by Figures 3 and 4.

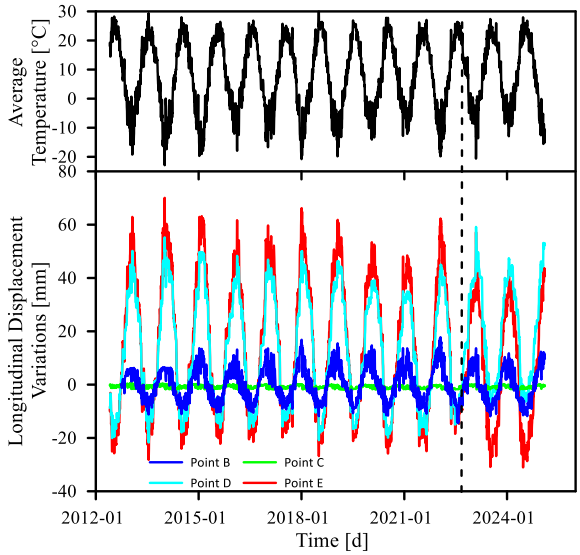

Figure 12. Box-girder longitudinal displacement relative to top of piers.

Under similar thermal loads year after year, the annual longitudinal displacement range decreases gradually from 2018 to 2022 (Figure 12), while top of pier rotation range is also decreasing (Figure 13). Measurements are linked together, and this result is in line with the gradual increase of mid-span deflection.

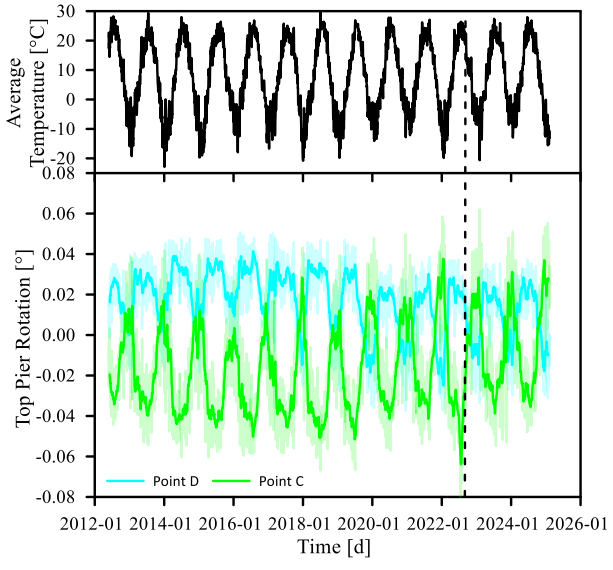

Figure 13. Top of piers rotation.

5.3 *Tracking of mid-span deflection*

Figure 14 shows mid-span daily average deflection as a function of time from November 2008, until February 2025. On the same figure, the blue dots represent bridge centre levelling and good agreement is observed.

Considering that temperature gradients have a greater influence on vertical deflection than average temperature, maximum mid-span deflection occurs early in winter. Regardless of creep, the annual deflection range is about 30 mm, close to the deflection caused by traffic serviceability loads (as confirmed by load tests). This result explains the significant variations that are observed in Figure 14, even with daily averages. This bridge is part of a freeway with an estimated average daily truck traffic of 1,600. The running average fit shown on the figure highlights the deflection trend over time.

Under similar thermal loads year after year, the mid-span deflection has been increasing since the sensors started recording. Furthermore, the process is accelerating.

Several factors have contributed to the increase in deflection at the centre of the bridge, including:

- concrete cracking under recurrent thermal loads and traffic loads.
- concrete shrinkage and creep.
- prestressing losses from steel relaxation, concrete long-term deformation, sleeve failure, bar corrosion, etc.

In addition to these phenomena, the bridge's response is influenced mainly by:

- the different thermal expansion coefficients of the various materials.
- the friction intrinsic to roller supports, which varies with temperature.
- the various thermal inertia of the structure's components (being a function of thickness and geometry).

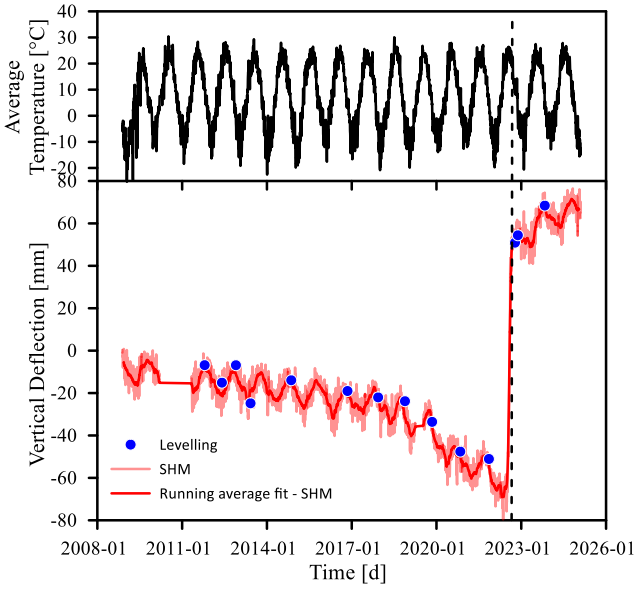

Figure 14. Mid-span deflection over the last 16 years.

In addition, 32 external prestressing tendons added to reinforce the structure in 1992 are exposed to ambient temperature inside the box girder, unlike the internal prestressing tendons, which are embedded in concrete.

DOI: 10.3217/978-3-99161-057-1-116

Ambient temperature in the box girder varies more rapidly than internal concrete temperature, and this fact justifies the multiple oscillations observed even on the running average display, and to the deflection which is not perfectly in phase with TM or GT.

As seen on Figure 14, the tensioning of the cable stays caused the observed rise at the centre of the central span. The centre continues to rise months after tensioning, indicating a probable subsequent creep recovery.

5.4 Tracking the breathing of groups of cracks using telescopic extensometers

As mentioned above, a total of eight telescopic extensometers were installed at longitudinal coordinates (length of the extensometer is indicated in parenthesis): two at coordinate 44 (6.5 m), two at coordinate 130 (6.5 m), two at coordinate 216 (6.5 m), one at coordinate 232 (5 m) and 239 (5 m) metres from B axis (Figure 1).

Figure 15 presents maximum seasonal response predictions at different locations where telescopic extensometers have been installed. These predictions have been made using the calibrated crack-free FE model. Two support conditions have been considered, whether the roller at point D is free to move horizontally or is partially restrained. Having the reference temperature set at 15°C, the annual mean temperature varies from 15°C (from Figure 6, the maximum temperature is about 30°C) to -35°C (the minimum temperature is approximately -20°C). As seen on Figure 6, the annual GT varies from 9°C/m in winter to -12°C/m during the summer.

Predictions indicate that a restraint at roller of point D (dark colours) reduces the annual total range of expected measurements. Also, a negative value is expected in summer for all sensors on the central span, meaning that these minimums are out of phase with mean temperature. For sensors of the side span (sections 232 and 239), expected maximum and minimum are in phase with mean temperature when roller at point D is restrained. With a free roller at D, maximum and minimum are out of phase with mean temperature. Depending on the stiffness of the restraint at the roller, a change in the sign of the bending moment can be observed from the central span to the approach span.

Figures 16 and 17 show twelve years of data recorded from extensometers 44 and 216. A positive recording corresponds to an extension of the sensor and crack opening. Note that in this figure, all sensors record their maximum value in winter, when the deck shortens. The contrary is noted in summer. Similar observations can be made at section 130.

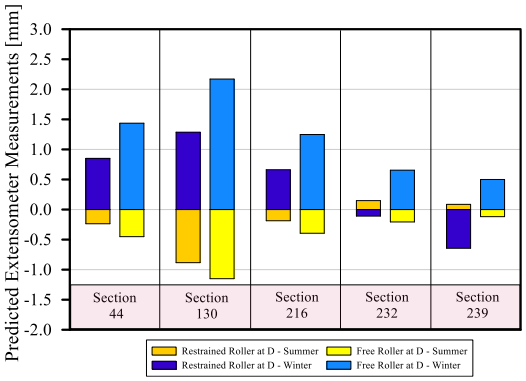

Figure 15. Maximum and minimum expected responses at five extensometer sections and different roller conditions.

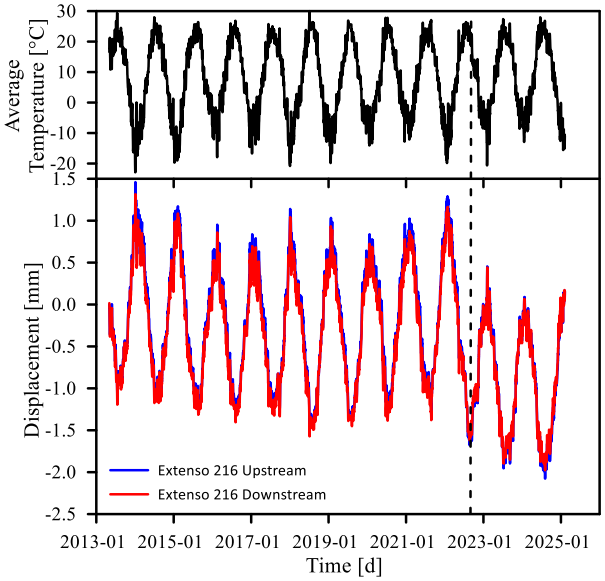

Figure 16. Recordings by extensometers 216.

At sections 44 and 216, measurements are therefore out of phase with concrete mean internal temperature, as predicted in Figure 15. However, the annual range of 2.5 mm is larger than expected with a crack-free model of the structure. This result seems to indicate the presence of active cracks. Recall that when a crack occurs, strain energy is released locally and thermal deformations along the prestressing bar are no longer uniformly distributed. Therefore, cracks may be considered as strain concentrators and if a sensor overlapped some of them, measurements can be amplified, especially when prestressing bars are not fully grouted.

Furthermore, sensors 44 and 216 experienced a permanent drop of approximately 0.75 mm following tensioning of the stay cables in September 2022. This result combines compressive strains and crack closures, since compression is induced in that area by the stay cable tensioning.

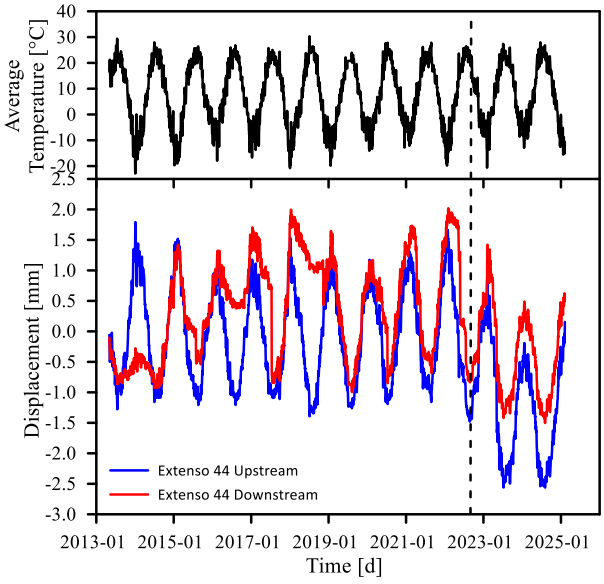

Figure 17. Recordings by extensometers 44.

Contrary to what can be seen in Figures 16 and 17, Figure 18 shows recordings from sensors 232 and 239 that are in phase

DOI: 10.3217/978-3-99161-057-1-116

with internal temperature variations. In that area, side-span predictions (Figure 15) made with the roller partially restrained are confirmed. However, the recorded annual measurement range shown in Figure 18 are much larger than the range expected with the crack-free model of the structure. Once again, active cracks may be present, and the compression resulting from cable stays tensioning induced permanent closing of these cracks, as shown on Figure 18.

As seen in Figure 18, Extenso_232 captured a permanent crack opening of 0.5 mm from the beginning of summer 2020 to fall 2021. This expansion is apparently not sufficient to eliminate the prestressing effect (decompressing crack lips). Also, as the stay cables were tensioned, Extenso_239 experienced a 0.75 mm shortening, which is in line with the negative bending moment expected in this portion of the rehabilitated bridge.

Once cracks are closed, additional compression in concrete induces a minute variation in extensometer response. In winter, the deck shortens (see Figure 3), and compression in concrete decreases up to a point where the cracks re-open. The opening (breathing) of these cracks is captured by the extensometers and the measurements are amplified accordingly, as shown in Figures 16, 17 and 18. It should be emphasized that total or partial horizontal restraint at point D is mandatory for such crack breathing. Mean temperature and thermal gradient are then contributing.

Also, it should be kept in mind that when cracks widen and concrete decompresses locally, the mechanical properties of the box girder at crack surroundings are locally modified and the axial and bending rigidities are significantly reduced. This may invalidate the estimate of local stress from strain measurements in the vicinity of cracks, as discussed later in this paper.

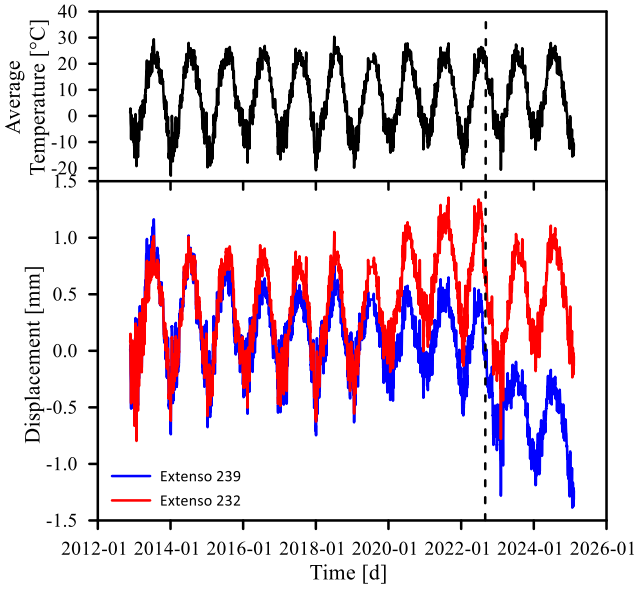

Figure 18. Recordings by extensometers 232 and 239.

5.5 Tracking of internal forces

In the case of the Grand-Mère Bridge, prestressing bars may be partially, if not fully, bonded to the surrounding concrete over most of their length. Consequently, the failure of a bar has generally a negligible effect upon vertical deflection and cannot be detected with strain sensors unless they are anchored close to the failure. However, cracking and delamination of large portions of concrete may significantly affect the intensity and distribution of the forces within the structure. Therefore, to grasp the effects of concrete deterioration, internal forces can be good estimators. It should be emphasized that measured strains (and resulting calculated stresses) do not represent the total strain (including the permanent state), but rather the strain increase that occurred after the sensors were installed. Also, it should be kept in mind that the average elastic modulus of prestressed reinforced concrete may depend on local conditions such as cracks, delamination, corrosion, and other disorders.

Figure 19 shows the variation of bending moments computed at measuring sections 47 (near pier B), 70, 135 (near the centre), 190 and 213 (near pier D). As shown in that figure, although there were no significant permanent load variations, the bending moment gradually decreased at sections 47 and 70 between fall 2008 and summer 2022. At the opposite side of the main span, measurements at section 190 (the counterpart section) also decreased, while a surprisingly slight increase has been observed at section 213. At the centre of the main span, bending moments increased, as we expected them to. Meanwhile, less significant decreases have been observed at sections 120 and 140 (not shown on the figure). Note the large variations observed after the tensioning of the cable stays in September 2022. These measurements have been useful in confirming the adequacy of the cable stay arrangement.

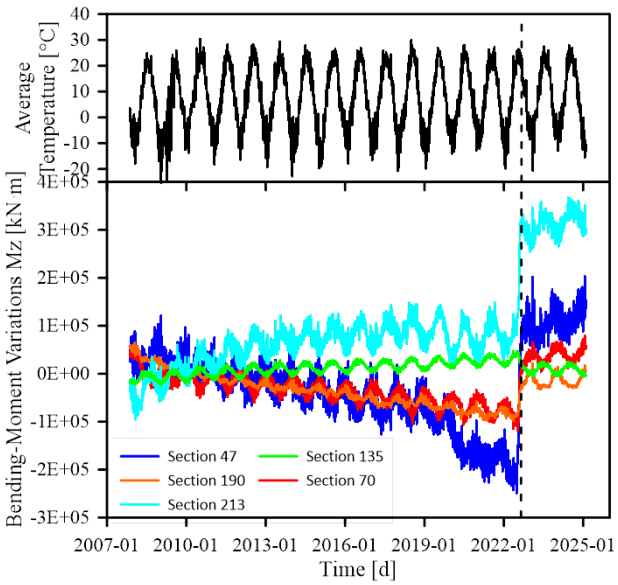

Figure 19. Bending-moment variations over time.

In a defect-free structure, bending moments vary according to the vertical deflection at the centre. To validate this statement and give insight to possible damage detection, a regression analysis has been performed between average daily bending moment M_z at a given cross-section and mean daily deflection at the centre as the explanatory variable. Figure 20 presents mean daily M_z at cross-section 47 as a function of mean daily deflection at the centre. The coefficient of regression for this distribution is equal to 0.85. Predictions from the defect-free numerical model are also presented. The comparison with the predicted behaviour indicates that for a given vertical deflection, the associated bending moment at section 47 is larger than expected.

DOI: 10.3217/978-3-99161-057-1-116

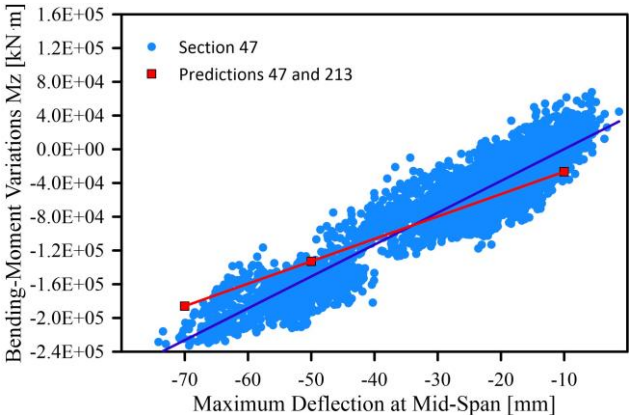

Figure 20. Bending-moment variations and predictions as a function of mid-span deflection.

The same regression analysis has been made with section 135 (near the centre) and section 213 (close to pier D). Figures 21 and 22 gather the results. At section 135, computed bending moments compare very well with predicted values, indicating that the bridge is behaving as expected under normal serviceability conditions. However, this is not the case at section 213 (Figure 22) where bending moments are not correlated with mid-span deflection (coefficient of regression for this distribution is less than 0.001). The comparison with the predictions (red line) makes this assessment apparent.

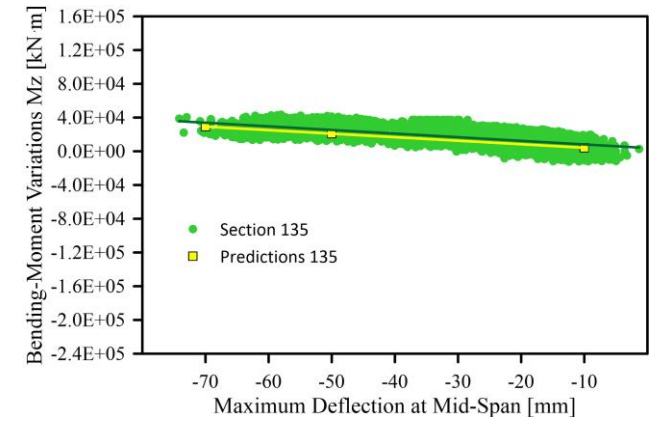

Figure 21. Bending moment variations and predictions as a function of mid-span deflection.

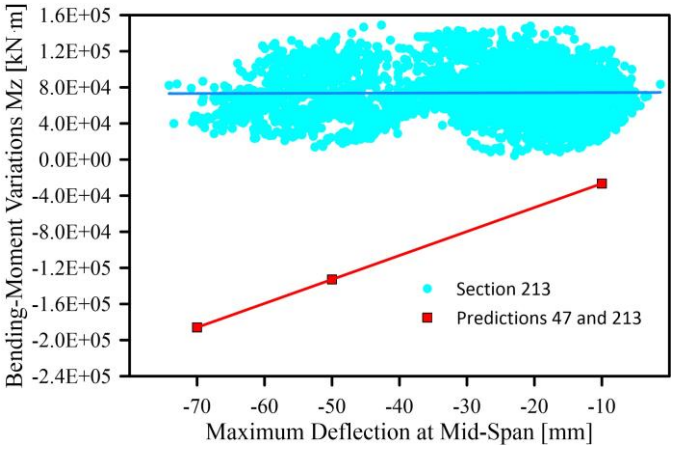

Figure 22. Bending moment variations and predictions as a function of mid-span deflection.

5.6 Tracking of mid-span box-girder torsional rotation

Figure 23 shows the recordings of the tiltmeter installed at the bridge centre, which measures box girder torsional rotation. A positive rotation is measured when the downstream web shifts downwards with respect to the upstream web, which may rise accordingly. In other words, a clockwise rotation around the bridge's longitudinal axis pointing east is assumed to be positive.

The data trend shown in Figure 23 indicates that girder torsional rotations are greatly correlated with internal temperature variations (the coefficient of regression being greater than 0.9). Also, an "event" may be noted around the end of April 2012, characterized by a rapid decrease of about 0.012° (from 0.0055° to -0.0065°) of the girder torsional rotation. Meanwhile, the internal temperature varies in the same way as in previous years. With permanent loads unchanged, this result suggests that structural damage took place, and the so-called event that occurred at the end of April 2012 may be the starting point of this apparent damage process. In fact, it can be shown that damage to a portion of a symmetrical cross-section (becoming unsymmetrical) induces such a torsional deformation. In Figure 19, the bending moment at section 213 became desynchronized from the bending moment at section 47 at approximately the same time.

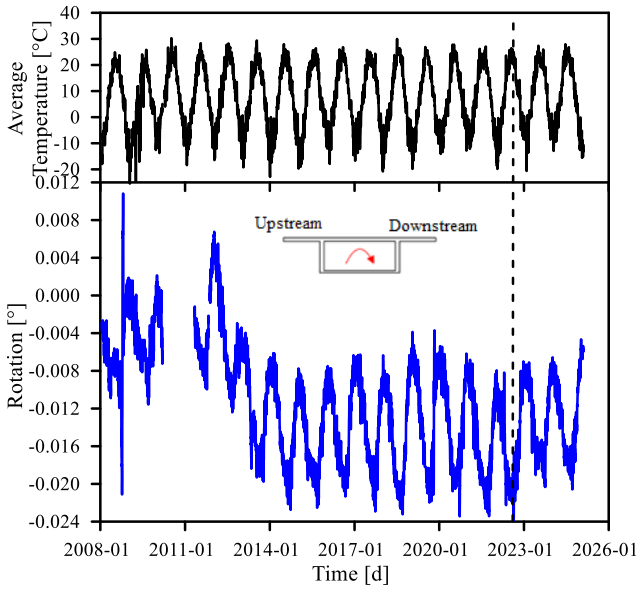

Figure 23. Box-girder torsional rotation at mid-span.

6 CONCLUSIONS

The structure under investigation was monitored for many years before it was strengthened. *In-situ* modal analysis and controlled load tests were conducted and recorded data were used to calibrate a representative numerical model of the bridge. Insights from a numerical model greatly helped bridge behaviour understanding and eventual damage detection. The model, in conjunction with long-term monitoring data, allowed for the identification of the following findings:

- Under ambient traffic conditions, 12 modal analyses have been carried out between 2003 and 2022. No significant changes were detected for the frequency of the first seven modes of vibration. Frequencies varied according to

DOI: 10.3217/978-3-99161-057-1-116

internal concrete temperature and the sudden slips that may occur at the roller as the bridge expands or contracts. The numerical model showed that the rollers at points B, D and E needs to be partially restrained to fits the measured frequencies.

- Free relative longitudinal movement was expected at the roller between the box girder and the top of D axis pier. Sensors showed that such movement was partially restrained, and that the piers bend according to internal temperature changes. The C axis pier is topped with pin bearings. Consequently, an horizontal force developed in the box girder between points C and D—compression in summer when the deck lengthens and traction in winter when the deck shortens. Incidentally, a permanent and progressive tilting was detected in these piers, a result that is in line with the observed permanent mid-span deflection.
- In addition to a slow and progressive permanent mid-span deflection, there was no unexpected or spontaneous sag increase over time. Creep and prestress losses were the dominant parameters contributing to the permanent sag of the main span.
- A permanent box-girder torsional rotation was detected at mid-span. Along with longitudinal stresses estimated at different sections along the deck, these observations revealed structural damage over the support at point D. Structural damage may take different forms, such as concrete cracking (accompanied by tension stress relaxation) or prestress loss (breaking of a tendon, loss of anchorage, corrosion), the latter being accompanied by compression stress relaxation.
- Telescopic extensometers were used to track the breathing of groups of cracks. Recorded data indicate that concrete in the vicinity of some cracks is decompressed when the temperature is low. In winter, the deck shortens and compression in concrete reduces up to a point where cracks widen. Crack openings are picked up by extensometers and the detected amplitude is larger than expected. The frozen bearings mentioned earlier are mandatory for this behaviour to occur, and residual prestressing forces are not sufficient to prevent crack breathing. Consequently, prestress loss causes a reduction of the structure's load-carrying capacity. Moreover, breathing cracks and concrete decompression cause larger stress cycles in prestressed tendons. This phenomenon promotes the premature failure of tendons, especially those located in the top flange, which is a corrosion-friendly environment (de-icing salts are spread on the roadway). Note that this diagnosis is achieved with no information on total applied stress, only with the help of long-term electronic monitoring data.
- The addition of cable stays was the solution chosen to strengthen the bridge. Since the cables have been tensioned, no progress has been observed in the damage processes of this structure.

Given the low relative stiffness offered by the stay-cable structure compared to that of the prestressed concrete box girder, this reinforcement:

- has little impact on the bridge's overall live load and thermal load responses (deflections, stress distribution and intensity, etc.).
- contributes to the bridge's structural redundancy, by enabling alternative load paths in the event of failure or excessive deformation of the box girder.
- introduces permanent stresses in the box girder that reduced the intensity of stresses caused by gravity loads, thus enabling some cracks to close and subsequent creep recovery.
- does not contribute to segment joint decompression, though new cracks were visually detected near the centre of the bridge.

Given the deficient design and erection problems affecting the strength and durability of this bridge, its reliability was questionable. Since the initial reinforcement of the structure, the electronic monitoring program presented has played a crucial role in managing this structure and keeping it in service for almost 50 years. The program has also enabled us to validate the structural effects induced by the reinforcement of the structure using stay cables.

ACKNOWLEDGMENTS

The authors would like to express their sincere thanks to all of those involved in this project, namely, Mr. Mathieu Lacoste, Eng., Ms. Geneviève David, Eng., and Mr. Éric L'Heureux, Tech., colleagues at the mobile laboratory team of the Direction de la gestion des structures of the MTMD, as well as the many dedicated engineers and technicians at Maurice-Centre-du-Québec regional office who have been involved in the project since 2001.

REFERENCES

[1] Massicotte, B., Picard, A., Ouellet, C., and Gaumond, Y. Strengthening of a Long Span Prestressed Segmental Box Girder Bridge. PCI Journal, 39(3), May-June, 1994.
[2] Ghali, A., Favre, R. and Elbadry, M. Concrete Structures: Stresses and Deformations: Analysis and Design for Sustainability. Fourth Edition, CRC Press, 2005.
[3] Bazant Z. P. and Qiang Y., Excessive Deflections of Record-Span Prestressed Box Girder, ACI Concrete International, Vol. 32, No. 6, June 2010.
[4] Bazant Z.P. and Baweja S. Creep and Shrinkage Prediction Model for Analysis and Design of Concrete Structures: Model B3. Adam Neville Symposium: Creep and Shrinkage—Structural Design Effects, ACI SP–194, A.Al-Manaseer, ed., Am. Concrete Institute, Farmington Hills, Michigan, 2000.
[5] Massicotte, B., Halchini, C. and Labbe, J. Evaluation of the Capacity of an Existing Steel Truss Bridge. IABSE Colloquium on "Remaining Structural Capacity," Copenhagen, Denmark, March 1993.
[6] Cremona, C. Qu'est-ce qu'une évaluation dynamique? Principes et méthodes. Revue européenne de génie civil, 9(1-2), 2005.
[7] Hou, X., Xueshan, Y. and Qiao, H. Using Inclinometers to Measure Bridge Deflection. Journal of Bridge Engineering, Vol. 10, Issue 5, 2005.
[8] Easa, S. M. Area of Irregular Region with Unequal Intervals. Journal of Surveying Engineering, Vol. 114(2), 1988.